BIOCHEMISTRY

 Volume 43, Number 38 September 28, 2004

Articles

Relocation of the Disulfonic Stilbene Sites of AE1 (Band 3) on the Basis of Fluorescence Energy Transfer Measurements†

Philip A. Knauf,*,‡ Foon-Yee Law,‡ Tze-Wah Vivian Leung,‡ and Stephen J. Atherton§

Department of Biochemistry and Biophysics and Center for Photoinduced Charge Transfer, University of Rochester, Rochester, New York 14642

Received June 30, 2004; Revised Manuscript Received July 22, 2004

ABSTRACT: Previous fluorescence resonance energy transfer (FRET) measurements, using BIDS (4-benzamido-4′-isothiocyanostilbene-2,2′-disulfonate) as a label for the disulfonic stilbene site and FM (fluorescein-5-maleimide) as a label for the cytoplasmic SH groups on band 3 (AE1), combined with data showing that the cytoplasmic SH groups lie about 40 Å from the cytoplasmic surface of the lipid bilayer, would place the BIDS sites very near the membrane's inner surface, a location that seems to be inconsistent with current models of AE1 structure and mechanism. We reinvestigated the BIDS−FM distance, using laser single photon counting techniques as well as steady-state fluorescence of AE1, in its native membrane environment. Both techniques agree that there is very little energy transfer from BIDS to FM. The mean energy transfer (E), based on three-exponential fits to the fluorescence decay data, is 2.5 ± 0.7% (SEM, $N = 12$). Steady-state fluorescence measurements also indicate <3% energy transfer from BIDS to FM. These data indicate that the BIDS sites are probably over 63 Å from the cytoplasmic SH groups, placing them near the middle or the external half of the lipid bilayer. This relocation of the BIDS sites fits with other evidence that the disulfonic stilbene sites are located farther toward the external membrane surface than Glu-681, a residue near the inner membrane surface whose modification affects the pH dependence and anion selectivity of band 3. The involvement of two relatively distant parts of the AE1 protein in transport function suggests that the transport mechanism requires coordinated large-scale conformational changes in the band 3 protein.

Band 3 or AE1 is a 101700 Da protein (*1*) in the human red blood cell, which catalyzes a very rapid exchange of Cl^- for HCO_3^-, thereby increasing the CO_2-carrying capacity of the blood (*2*−*5*). In addition to being physiologically important in red blood cells, AE1 is a member of the AE gene family (*6*−*8*), which includes proteins that function as anion exchangers in a variety of cells and tissues, such as kidney, white blood cells, epithelia, and neurons, where they play a role in cell pH and volume regulation. AE1 catalyzes an obligatory one-for-one exchange of anions and thus serves as a model for exchange (antiport) systems.

Kinetic studies have revealed that the system probably works by a ping-pong mechanism, in which the protein can be in a form with the transport (substrate) site facing either inward (E_i) or outward (E_o) and in which chloride or other

† Supported by NIH National Institute for Diabetes, Digestive and Kidney Diseases (NIDDK) Grant R01 DK-27495 and NSF Science and Technology Center Grant CHE-9120001.

* Corresponding author. Tel: 585-275-5459. Fax: 585-273-4746. E-mail: philip.knauf@rochester.edu.

‡ Department of Biochemistry and Biophysics, University of Rochester.

§ Center for Photoinduced Charge Transfer, University of Rochester.

10.1021/bi048622a CCC: $27.50
Published on Web 08/27/2004

substrate binding facilitates the transition between these two conformations (*2*−*4*). Although the primary sequence of AE1 has been known for over 15 years, and although a low-resolution 3D structure has been obtained by electron diffraction analysis of 2D crystalline arrays (*9*), little is known about the location and nature of the mechanism in the protein that gives rise to the one-for-one anion exchange.

The identification of band 3 or AE1 as the anion exchanger was first proposed on the basis of labeling experiments with the disulfonic stilbene (DS)[1] probes, such as DIDS (4,4′-diisothiocyanostilbene-2,2′-disulfonate) and H_2DIDS (4,4′-diisothiocyanodihydrostilbene-2,2′-disulfonate). Both of these act as affinity labels, with high-affinity noncovalent binding preceding the covalent reaction (*10*, *11*). Increasing concentrations of the substrate, Cl^-, reduce the inhibitory potency of H_2DIDS (*12*), as expected if H_2DIDS competes with Cl^- for binding to the external-facing anion transport site. Thus, it seemed that disulfonic stilbenes could be useful probes for localizing the substrate binding site in the AE1 protein.

Since then, several kinds of experiments have seriously challenged the concept that the stilbenedisulfonates are competitive inhibitors of Cl^- exchange and, thus, that the DS sites are equivalent to the Cl^- transport sites. Mutations that strongly influence DS binding have little or no effect on Cl^- affinity (*13*), interactions between Cl^- and DS are observed which are not compatible with a simple competition (*14*, *15*), and external DS can bind to the form of AE1 with the transport site facing inward (*16*). Nevertheless, it is still true that DS such as DIDS and DNDS (4,4′-dinitrostilbene-2,2′-disulfonic acid) greatly interfere with Cl^- binding to AE1 (*17*), and the inhibitory potency of DS is far greater when they are at the external side of the membrane than when they are located internally (*18*). Further, the binding of at least some DS is highly selective for the form of AE1 with the transport site in the external-facing, unloaded form (E_o) (*16*, *19*, *20*). Thus, the DS seem to bind to a region of the AE1 protein that is intimately involved in the protein conformational change that results in anion translocation, so these labels can provide very useful information concerning the location of part of the transporting mechanism within the AE1 protein.

Many years ago, Rao et al. (*21*) used fluorescence resonance energy transfer (FRET) to measure the distance between the DS sites and SH groups (now known to be Cys-201 and Cys-317) located in the cytoplasmic, N-terminal segment of AE1, which can be selectively labeled by fluorescein maleimide (FM). As a fluorescent label for the DS site, they used 4-benzamido-4′-isothiocyanostilbene-2,2′-disulfonate (BIDS). By observing donor (BIDS) quenching or stimulated emission of the acceptor (FM), they measured an energy transfer efficiency of 0.46−0.47, corresponding to a distance of 34−42 Å, depending on which assumptions were used regarding the number of acceptors and the relative orientation of donor and acceptor transition dipoles. This was a seminal finding, because it showed that the DS sites were closer to the cytoplasmic SH groups than the thickness of the membrane (∼45 Å), demonstrating that the DS sites, and thus it was thought the transport sites, were located within the membrane bilayer, rather than at the external surface.

Thevenin et al. (*22*) used FRET as well as a novel radioisotope technique to determine that the distance between the principal cytoplasmic SH site labeled by FM (Cys-201, shown by yellow circles in Figure 1) and the inner surface of the membrane bilayer (indicated in blue in Figure 1) is about 40 Å. When combined with the FRET measurement of the distance between the SH cluster and the DS site (34−42 Å), these data place the DS site very near to the level of the lipid headgroups of the inner half of the bilayer (Figure 1; BIDS at this location is shown by the magenta cross-hatched rectangle). Another residue, Glu-681, which is the site of reaction with Woodward's reagent K (WRK) and which is thought to play an important role in AE1-mediated transport of protons with sulfate, is also located near the inner half of the bilayer (orange circles in Figure 1), on the basis of biotin maleimide labeling studies of single-cysteine AE1 mutants. Location of the DIDS and WRK labeling sites close to each other near the inner surface of the lipid bilayer would be consistent with a model in which anions diffuse through a long access channel from the outside to the transport site and anion transport across the diffusion barrier takes place within a very small portion of the AE1 membrane domain located right next to the cytoplasm.

Such a locus for the DS sites seems very unlikely in view of evidence that the DS H_2DIDS reacts covalently with two amino groups, Lys-539 and Lys-851 (*23*). There is strong recent evidence that Lys-851 is located immediately next to an extracellular loop of AE1. Both biotin maleimide (*24*) and the positively charged reagent MTSET [[2-(trimethylammonium)ethyl]methanethiosulfonate] (*25*) covalently label the sites Ser-852 and Thr-853 in AE1 mutants with cysteine substituted for these residues, expressed in HEK293 cells. Lys-539 is also thought to be near the extracellular end of a transmembrane helix of AE1, and natural mutations of two AE1 residues not far from Lys-539, Pro-548 (*26*) and Thr-552 (*27*), give rise to antibodies against intact red blood cells, indicating that these sites are externally exposed. Models for AE1 topology based on this and other evidence agree that the DS-reactive parts of AE1 are located near the external surface of the membrane (*4*, *28*, *29*). In the very likely case that the analogous DS BIDS also reacts with one or both of these sites, it would not be possible for the BIDS molecule, which is only about 22 Å long (*30*), to have its fluorophore located at the level of the inner bilayer surface.

[1] Abbreviations: 150 KH, 150 mM KCl, 24 mM sucrose, and 20 mM Hepes, pH 6.9 at room temperature; 5P8, 5 mM sodium phosphate and 1 mM EGTA, pH 8 at room temperature; 5P8Cl, 5P8 supplemented with 135 mM NaCl and 0.1 mM NaEDTA; 5P7.4, 5 mM sodium phosphate, pH 7.4 at room temperature; *a*, fractional Cl^- exchange activity; *B*, concentration of free BIDS; B_t, total concentration of BIDS; b3B, concentration of BIDS bound to band 3; $b3_t$, total band 3 concentration; BADS, 4-benzamido-4′-aminostilbene-2,2′-disulfonate; BIDS, 4-benzamido-4′-isothiocyanostilbene-2,2′-disulfonate; BSA, bovine serum albumin; DADS, 4,4′-diaminostilbene-2,2′-disulfonic acid; DBDS, 4,4′-dibenzamidostilbene-2,2′-disulfonate; DIDS, 4,4′-diisothiocyanostilbene-2,2′-disulfonate; DNDS, 4,4′-dinitrostilbene-2,2′-disulfonic acid; DS, disulfonic stilbene; DTT, dithiothreitol; EM, eosin-5-maleimide; FM, fluorescein-5-maleimide; FRET, fluorescence resonance energy transfer; H_2DIDS, 4,4′-diisothiocyanodihydrostilbene-2,2′-disulfonate; hct, hematocrit; IC_{50}, concentration which inhibits transport by 50%; *k*, rate constant for ^{36}Cl exchange; k_c, control rate constant for ^{36}Cl exchange; K_d, dissociation constant for BIDS binding to band 3; KIOV's, KI-stripped inside-out vesicles; NBD, 4-nitrobenz-2-oxa-1,3-diazole; PBS, 25 mM NaH_2PO_4, 1 mM EDTA, and 95 mM NaCl, pH 7.4 at room temperature; PMSF, phenylmethanesulfonyl fluoride; R_0, distance in angstroms at which energy transfer efficiency is 0.5; SDS, sodium dodecyl sulfate; TLCK, L-1-chloro-3-(4-tosylamido)-7-amino-2-heptanone hydrochloride.

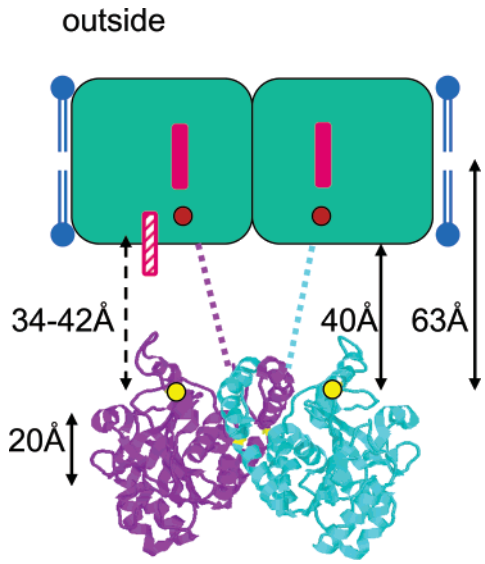

FIGURE 1: Schematic diagram of the AE1 dimer in red cell membrane. The membrane domain of the AE1 dimer (approximately residues 405−880) is shown in green at the top, with the membrane bilayer indicated in blue. Dimensions are based on the 20 Å resolution structure of Wang et al. (*9*). A portion of the cytoplasmic domains seen in the crystal structure (*62*) (residues 55−356) is shown toward the bottom, with Cys-201 residues indicated by yellow circles. The structure of the cytoplasmic domain at neutral pH is likely to be somewhat altered from the crystal structure at pH 4.8, and the orientation of the structure relative to the membrane plane is somewhat uncertain, but this does not affect the FRET data concerning the location of Cys-201. Because of the very limited structural information on the intervening region between the part of the cytoplasmic domain seen in the crystal structure and the membrane domain, this is shown by dashed lines. Data of Rao et al. (*21*) indicated a distance of 34−42 Å (dashed arrow) between Cys-201 and BIDS. Together with data indicating that Cys-201 is located about 40 Å from the cytoplasmic side of the membrane bilayer (*22*), this places the BIDS label at the cytoplasmic surface of the membrane domain (indicated by the magenta crosshatched rectangle), near the Glu-681 location, shown by the orange circles. BIDS is shown with its chromophore (approximately 16 Å long) oriented vertically in the membrane, the worst case scenario in terms of the ability of FRET to specify its location relative to the axis normal to the membrane surface. Because certain DS, such as H_2DIDS, are able to cross-link residues that are unlikely to be at very different levels within the membrane, it is likely that the orientation is more horizontal (*4*, *75*). Data in this paper indicate a much larger distance between BIDS and Cys-201, approximately 63 Å or greater, which places the BIDS sites (indicated by the solid magenta rectangles) near the center of the membrane or in its outer half, far from the Glu-681 site.

The earlier BIDS−FM FRET measurements were made by steady-state fluorescence, possibly without acceptor background correction, or by modulation measurements of lifetime that may not have had sufficient time resolution to accurately determine lifetimes as short as that of BIDS. Also, most of the data were obtained with detergent-solubilized AE1, which may have undergone conformational changes. We therefore reinvestigated the BIDS−FM distance, using both steady-state fluorescence of AE1 and laser single photon counting techniques to measure energy transfer efficiency, while maintaining AE1 in its native membrane environment. The data we obtained are incompatible with the conclusions of Rao et al. and suggest instead that the DS sites are located much farther from the cytoplasmic SH cluster. This relocation of the DS sites implies that the transporting mechanism involves conformational changes of widely separated portions of the AE1 domain, in agreement with models based on recent crystal structures of bacterial anion exchangers (*31*, *32*). Portions of this work have appeared previously in abstract form (*33*).

EXPERIMENTAL PROCEDURES

Cell Preparation. Blood from apparently healthy adult donors, who had given informed consent, was drawn into heparinized vacutainers and then washed three times with ice-cold 150KH (150 mM KCl, 24 mM sucrose, and 20 mM Hepes, pH 6.9 at room temperature, unless otherwise specified). The buffy coat was removed, and the cells were resuspended to 50% hematocrit (hct) in 150KH.

Preparation of Ghosts and KI-Stripped Inside-Out Vesicles (KIOV's). Ghosts were prepared (*34*) by lysing packed cells at 0 °C in 5P8 (5 mM sodium phosphate and 1 mM EGTA, pH 8 at room temperature) containing 0.2 mM phenylmethanesulfonyl fluoride (PMSF). After centrifugation at 30000*g* at 4 °C for 7 min in a Dupont Instruments RC5 refrigerated centrifuge, the supernatant and the sticky pellet at the bottom were removed by aspiration. Ghosts were then washed in 5P8 multiple times until white. KIOV's were prepared by the method of Bennett (*35*). The protein content of ghosts or KIOV's was determined by the BCA protein assay (Pierce), using bovine serum albumin as a standard.

Trypsin or Chymotrypsin Cleavage. The procedures of Jennings (*36*) were used for enzyme treatments. BIDS-labeled red cells at 25% hct in 150KH, pH 7.4 at 37 °C, were treated with chymotrypsin at 1 mg/mL in the extracellular volume at 37 °C for 1 h. The reaction was stopped by ice-cold 150KH containing 0.2 mM PMSF and 0.2% BSA. The cells were washed two more times in 150KH. Ghosts at 1 mg/mL in 5P8 were cleaved by 50 μg/mL trypsin at 0 °C for 5 min, except where otherwise indicated. The reaction was inhibited by adding 50 μg/mL TLCK (L-1-chloro-3-(4-tosylamido)-7-amino-2-heptanone hydrochloride) followed by three washes in 5P8.

Synthesis of BIDS. BADS (4-benzamido-4′-aminostilbene-2,2′-disulfonate) was prepared (*37*) by adding an equimolar amount of benzoyl chloride dropwise to a solution of DADS (4,4′-diaminostilbene-2,2′-disulfonic acid) and a 3-fold molar excess of $NaHCO_3$ in water at room temperature. After 4.5 h reaction, 6 N HCl was added to reduce the pH to 1. The precipitate was collected and dissolved in methanol at 60−70 °C and concentrated to $^1/_{10}$th its volume, and 5 volumes of diethyl ether were added to precipitate BADS. The product was dissolved in pyridine−acetic acid−water (10:1:40), applied to a silica gel column, and eluted with the same solvent. The fractions containing BADS were identified by thin-layer chromatography, pooled, concentrated, and recrystallized from methanol−water (10:1) and then from water. The UV spectrum showed the expected peak at 342−344 nm.

BIDS was prepared (*21*, *38*) by dissolving 0.2 mmol of BADS in 3.5 mL of 1% NaCl and then adding 100 μL of thiophosgene with vigorous stirring. After 3 h reaction, excess thiophosgene was removed by three 4 mL extractions with diethyl ether. The yellow precipitate was recrystallized from 1% NaCl and dried. There was a UV peak at 338−340 nm as expected and a fluorescence emission peak at 428 nm with excitation at 350 nm. All syntheses were

performed by Dr. Xiuzhi Wang in the Department of Chemistry.

BIDS dissolved in 5P8 had an ϵ at 339 nm of 33800 M^{-1} cm^{-1}, based on a molecular weight of 516 for the acid form of BIDS. This is lower than the ϵ of 62000 M^{-1} cm^{-1} reported by Rao et al. (*21*), suggesting that there might be some impurities or inert material in the BIDS sample. The principal impurities that could arise from synthesis are DBDS (4,4′-dibenzamidostilbene-2,2′-disulfonate) or DIDS (4,4′-diisothiocyanostilbene-2,2′-disulfonate). DBDS binds reversibly and so would not be expected to be found in ghosts from labeled cells; DIDS reacts irreversibly but has little optical absorbance and fluorescence. If some DIDS were present in the BIDS sample, so that some of the band 3 was labeled by DIDS rather than BIDS, this would reduce the total donor fluorescence but should not affect the energy transfer from the BIDS donors to internal FM. Thus, possible impurities in the BIDS are very unlikely to explain our results.

BIDS Labeling. Cells were washed once in 150KH, pH 8 (150KH, pH = 8 at 37 °C). BIDS from a 1 mM stock in water was added to 20−50% cells at a final concentration of 24−300 μM in the extracellular volume, as indicated. (All concentrations are expressed in terms of extracellular volume.) At the end of 1 h incubation at 37 °C, at least four volumes of ice-cold 150KH containing 1% BSA was added to the cell suspension, which was spun down and washed three more times in 150KH without BSA. Alternately, cells were labeled with BIDS according to the method of Rao et al. (*21*). Portions of the BIDS-labeled and control cells were incubated with ^{36}Cl, and Cl^- exchange was measured at 0 °C as described previously (*39*, *40*).

To determine the dissociation constant for reversible BIDS binding, we examined the effects of short exposures to BIDS on the rate constant for Cl^- exchange, *k*, at 0 or 21 °C, by adding BIDS directly to the medium in which the cells were suspended for flux measurements. For experiments at 21 °C, cells were pretreated with DIDS to reduce the control *k* value to a level that would permit measurement of the time constant by the rapid syringe filtration method used at 0 °C.

FM Labeling of Cells or Ghosts. Cells were labeled at externally accessible sites with FM (FM_o) as described by Bicknese et al. (*41*). Briefly, 50% cells in PBS (25 mM NaH_2PO_4, 1 mM EDTA, and 95 mM NaCl, pH 7.4 at room temperature) were incubated with a 1 mM final concentration of FM for 1 h at 23 °C. The reaction was stopped by diluting 10-fold with PBS supplemented with 1 mM cysteine and 5 mg/mL BSA. The labeled cells were washed three times in PBS and once in 150KH.

Ghosts were labeled by the method of Thevenin et al. (*22*), except at pH 8 instead of pH 7.4. Ghosts at a protein concentration of 1 mg/mL in 5P8 supplemented with 135 mM NaCl and 0.1 mM NaEDTA (5P8Cl) were treated with 50 μM FM for 30 min at 0 °C. DTT (dithiothreitol) was added at 0.2 mM final concentration to stop the reaction. The FM-labeled ghosts, which are primarily labeled at internally accessible sites (FM_i), were then washed three times in 5P8. Alternately, as indicated, ghosts were labeled with FM by the method of Rao et al. (*21*).

Measurement of Labeling. The FM-labeled ghosts or KIOV's were solubilized in 1% SDS, electrophoresed in a 12% sodium dodecyl sulfate−polyacrylamide gel (*42*), and scanned in a FluorImager 575 (Molecular Dynamics). To calculate the percent FM in band 3, the fluorescence in band 3 was compared to the total fluorescence in the gel lane with background subtracted. Total FM labeling was determined from the optical density at 491 nm, measured in a Shimadzu UV1600U spectrophotometer, of ghosts solubilized in 0.2% SDS, using an ϵ value of 55000 M^{-1} cm^{-1} (*21*). The number of moles of FM per mole of band 3 was calculated by multiplying the percent FM in band 3 by the total amount of FM per mole of band 3, assuming that b3 comprises 25% of the total ghost protein (*43*) or 60% of the total protein of KIOV's, using 101.7 kDa as the band 3 molecular mass (*1*).

BIDS labeling selectivity was also assessed by electrophoresis on 12% SDS linear polyacrylamide gels followed by observation in a UV light box (Chromato-Vue transilluminator, Model C-62; Ultra Violet Products, Inc.) with excitation at 366 nm. Total BIDS binding to ghost membranes was measured by absorption at 339 nm in 5P8 containing 0.2% SDS using a molar extinction coefficient of 51000 M^{-1} cm^{-1}(*21*).

Determination of the Number of BIDS Binding Sites by Stoichiometric Inhibition of Cl^- Exchange. A maximal estimate for the number of BIDS binding sites was obtained by a method similar to that used previously with a high-affinity oxonol dye (*44*). Cells at 20% hematocrit were treated with concentrations of BIDS (or DIDS, for comparison) less than or slightly greater than the concentration of band 3 sites for 1 h at 37 °C in 150KH, pH 8 at 37 °C. A sample was taken for determination of the number of red cells by spectrophotometry of a lysate in water at 549 nm, taking the molar extinction coefficient for hemoglobin as 12060 M^{-1} cm^{-1} and the hemoglobin content as 30 pg per cell. Cells were washed once with 150KH containing 1% BSA and three times without BSA, and then Cl^- exchange was measured at 0 °C as described previously (*39*, *40*). The fractional activity of Cl^- exchange was plotted against the total number of BIDS (or DIDS) molecules present per cell in the labeling suspension.

Although this method measures irreversible inhibition due to covalent binding of BIDS or DIDS, for disulfonic stilbenes the covalent reaction is preceded by a reversible high-affinity binding. The fractional activity remaining after exposure to the inhibitor, *a*, can be approximated by the equation for single-site reversible binding:

$$a = 1/(1 + B/K_d) \quad (1)$$

where *B* is the concentration of free BIDS in the solution and K_d is the apparent dissociation constant for BIDS binding to band 3. In this case, K_d is not equal to the reversible binding constant but rather is a phenomenological constant that is dependent on the time and rate of the covalent reaction. For labels such as BIDS and DIDS, where K_d is very small, this has little effect on the fits to the data. *B* can be expressed in terms of the total concentration of BIDS added, B_t, and the concentration of BIDS bound to band 3, b3B:

$$B = B_t - \mathrm{b3B} \quad (2)$$

and similarly b3B can be expressed in terms of the total band 3 concentration in the labeling suspension, $b3_t$, and the fractional activity, a ($=1 - b3B/b3_t$):

$$b3B = (1 - a)b3_t \quad (3)$$

Substituting (2) and (3) into (1), we obtain a quadratic equation:

$$b3_t a^2 + (B_t - b3_t + K_d)a - K_d = 0 \quad (4)$$

whose solution is

$$a = \frac{b3_t - K_d - B_t + \sqrt{(b3_t - K_d - B_t)^2 + 4b3_t K_d}}{2b3_t} \quad (5)$$

Equation 5 was fitted by nonlinear least squares to the data for a versus B_t to determine $b3_t$. The total number of BIDS binding sites was determined from $b3_t$, Avogadro's number, and the concentration of red cells in the labeling suspension. This method assumes that every molecule of BIDS (or DIDS) in the solution contributes to the inhibition of Cl^- exchange; thus it gives a maximal estimate for the number of binding sites present.

Steady-State Fluorescence Measurements. Fluorescence spectra were acquired and corrected with a modified Photon Technologies, Inc. (Monmouth Junction, NJ) Alphascan fluorometer, using Felix software supplied by the manufacturer.

Quantum Yield and R_0 Determination. The quantum yield of BIDS bound to ghosts was determined in 5P8 at room temperature by comparing the quantum yield to that of fluorescein in 0.1 M NaOH, which was taken as 0.92. R_0 was determined from the fluorescence emission curve for BIDS-labeled ghosts and the absorbance spectrum for FM-labeled ghosts using $\epsilon = 55000\ M^{-1}\ cm^{-1}$ for FM-cysteine (*21*) and taking the refractive index as 1.34 and κ^2 as $^2/_3$ (*45*, *46*).

Fluorescence Lifetime Measurements. BIDS fluorescence lifetimes were measured by the single photon counting method at the Center for Photoinduced Charge Transfer in the Department of Chemistry (*47*) at room temperature with ghosts at a concentration of 0.2 mg of protein/mL in 5P8. For comparison, a BIDS−lysine standard was prepared by reacting 1 mM BIDS in 5 mM lysine at pH 9 for 2 h at room temperature (*21*). A mode-locked Nd:YLF laser produced pulses at 1053 nm, which were frequency doubled in a KTP (potassium titanyl phosphate) crystal. The pulses were used to synchronously pump a Coherent 700 series pyridine-1 dye laser, with a Coherent 7220 cavity dumper, used to reduce pulse repetition rate and decrease pulse width to about 6 ps. The output at 700 or 720 nm was frequency doubled in a BBO (beta barium borate) crystal to produce 350−360 nm light for excitation. Fluorescence at 440 or 442 nm was collected at right angles using a SPEX monochromator and a microchannel plate photomultiplier. The instrument response function (IRF) was obtained from the light scattering signal at the excitation wavelength. Data were acquired and fitted by least squares, using FLA900 software (Edinburgh Analytical Instruments), with correction for the IRF, to an equation for two- or three-exponential decay:

$$I(t) = \sum_{i=1}^{n} \alpha_i \exp(-t/\tau_i) \quad (6)$$

where $I(t)$ is the fluorescence intensity (photons) and α_i and τ_i are the amplitudes and time constants for the n individual exponential components. Deviations of the experimental points from the best fit line were expressed as weighted residuals: (actual counts − calculated counts)/(calculated counts)$^{1/2}$ (*48*).

Calculation of Energy Transfer Efficiency, E, and Donor−Acceptor Distance, R. In cases such as the present observations, where the individual components of the decay curve cannot be accurately resolved, because of the mathematical difficulties in fitting multiple exponential functions, effects of energy transfer can be measured from changes in the average lifetime, $\bar{\tau}$, given by (see p 130 of ref *49*)

$$\bar{\tau} = \sum_i \alpha_i \tau_i^2 / \sum_i \alpha_i \tau_i \quad (7)$$

E was determined from donor (BIDS) lifetime measurements from the equation (*50*):

$$E = 1 - \bar{\tau}_{DA}/\bar{\tau}_D \quad (8)$$

where τ_D is the lifetime of the donor and τ_{DA} is the lifetime of the donor in the presence of acceptor. Alternately, E was determined from steady-state measurements as (*50*)

$$E = 1 - F_{DA}/F_D \quad (9)$$

where F_D is the fluorescence of the donor in the absence of acceptor and F_{DA} is the fluorescence with acceptor present. These E values were used to determine the distance between the donor and acceptor from the equation (*51*):

$$R = R_0 \sqrt[6]{(1 - E)/E} \quad (10)$$

RESULTS

Kinetics of the BIDS Reaction. To have sufficiently bright fluorescence to analyze, it is preferable that the BIDS labeling of AE1 be as complete as possible. Figure 2 shows the time course of the irreversible inhibition of Cl^- exchange at pH 8 by 28.6 μM BIDS at 37 °C. The data fit quite well to a single exponential with a rate constant of 0.073 ± 0.003 min^{-1} corresponding to a half-time of 9.5 min. Since band 3 is known to be in the form of dimers or higher oligomers in the red cell membrane (*52*−*54*), reaction of BIDS with one band 3 monomer might decrease the reactivity of the adjacent monomer in a band 3 dimer. A two-exponential function gave a very slightly better fit, but with the faster component amounting to only 12% of the total, inconsistent with the dimer interaction model. The very good fit of the data to a single exponential indicates that, if there is any effect of reaction with one monomer on the adjacent monomer, the effect is very small.

If BIDS acts as an affinity label like other disulfonic stilbenes (*11*), with reversible binding preceding the covalent reaction step, the reaction rate should approach a plateau when the reversible binding reaches saturation. To determine

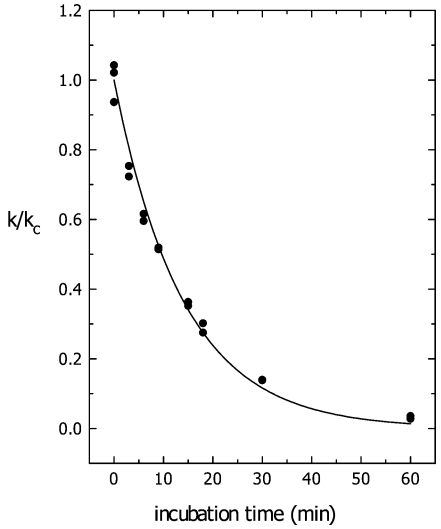

FIGURE 2: Time course of BIDS inhibition of Cl^- exchange. Red cells at 33% hct were exposed to 28.6 μM BIDS in 150KH at pH 8 for various times at 37 °C. The reaction was stopped by adding ice-cold 150KH with 1% BSA, and then the cells were washed three times in 150KH. Cells were incubated with $^{36}Cl^-$ at room temperature for 15 min and placed on ice, and the rate constant for $^{36}Cl^-$ exchange (k) was measured at 0 °C as described in Experimental Procedures. The rate constants were divided by the control rate constant (k_c) and plotted against time. The line shows the best fit to the equation $k/k_c = 1 - \exp(-k_r t)$, where k_r is the rate constant for the reaction of BIDS with AE1.

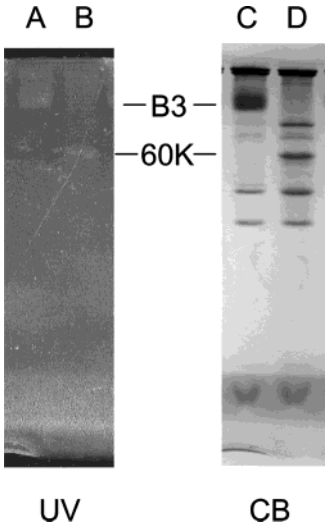

FIGURE 3: Polyacrylamide gel electrophoresis of ghosts from BIDS-labeled cells. Cells were treated with 212 μM BIDS (concentration in the extracellular medium) for 90 min at 37 °C. Ghosts were solubilized in 0.2% SDS and electrophoresed on 12% polyacrylamide gels as described in Experimental Procedures. The left-hand panel (UV) shows the fluorescence image obtained by long-wave UV excitation on a Chromato-Vue transilluminator, Model C-62 (Ultra Violet Products, Inc.). The left channel (A) shows ghosts from cells labeled with BIDS; the right channel (B) shows the result when cells were treated with chymotrypsin (1 mg/mL for 60 min at 37 °C). The right panel (CB) shows Coomassie Blue stained gels of the same samples: (C) control and (D) chymotrypsin. Note that the very faint fluorescence runs at the position of band 3 in the ghosts from BIDS-labeled cells and at the position of the 60 kDa N-terminal band 3 fragment generated by chymotrypsin cleavage.

the dissociation constant for the reversible binding, we examined the effects of short exposures to BIDS on the rate constant for Cl^- exchange, k, at 0 or 21 °C as described in Experimental Procedures. BIDS concentrations were determined by weight, assuming 100% purity. Data (not shown) were fitted to the equation for single-site reversible inhibition, $k = k_c/(1 + [\text{BIDS}]/\text{IC}_{50})$, where k_c is the control rate constant and IC_{50} is the concentration of BIDS that gives 50% inhibition of the flux. The IC_{50} was 57 ± 3 nM at 0 °C and 62 ± 18 nM at room temperature. The IC_{50} at 0 °C is similar to that for the disulfonic stilbene with the highest known affinity for AE1, DIDS (31 nM) (*55*). Thus it is likely that BIDS binds to the same high-affinity DS site.

Because there was very little effect of temperature on the IC_{50}, at 37 °C the IC_{50} is probably also low. Thus it is not necessary to use high BIDS concentrations for the reaction (although for complete labeling of band 3 at the high hematocrits used in most experiments, it is obviously necessary to have more BIDS present than AE1 molecules). As expected for an affinity-labeling mechanism, in which a high-affinity reversible binding precedes the covalent reaction, at 37 °C 70 μM BIDS inhibited Cl^- exchange to the same extent as did 200 μM BIDS (data not shown).

Specificity and Stoichiometry of BIDS Labeling. For BIDS to provide reliable information about the structure of AE1, it is necessary that the BIDS labeling be as specific for AE1 as possible, that is, that most or all of the BIDS molecules be bound to AE1. We first examined labeling specificity by reacting intact red blood cells with 297 μM BIDS for 1 h at 37 °C and then analyzing the membrane proteins from these cells on SDS−polyacrylamide gels. Cl^- exchange flux was inhibited by over 97%, indicating that nearly all band 3 molecules had reacted with BIDS, as expected from the reaction kinetics described above. Because of the very low quantum yield of BIDS in aqueous media, it was not possible to quantitate the amount of BIDS in various regions of SDS−polyacrylamide gels of ghosts from BIDS-labeled cells. When visualized under UV light (Figure 3), only a single faint fluorescent band could be detected in a position corresponding to band 3; after chymotrypsin treatment of intact cells, this label was found in the position of the 60 kDa fragment of band 3. These data indicate that no other single membrane component is labeled by BIDS to the same extent as AE1, but they do not provide quantitative data to rule out the possibility that a large fraction of the BIDS, perhaps even more than the amount bound to AE1, could be distributed among a number of membrane proteins.

Because of the very high affinity of BIDS as an inhibitor of Cl^- exchange, it is possible to determine the maximum number of BIDS molecules that are interacting with red blood cells by exposing cells to different amounts of BIDS and measuring the inhibition of Cl^- exchange, assuming that all of the BIDS molecules present contribute to the inhibition. The fraction of Cl^- exchange remaining is plotted against the total number of BIDS molecules added (Figure 4), and the data are fitted to a model which assumes that transport inhibition is a linear function of the number of BIDS bound per band 3 molecule and that there is a finite dissociation constant (K_d) for BIDS binding (see Experimental Procedures). Since binding of BIDS to all sites, whether or not this binding produces inhibition of Cl^- exchange, depletes the limited supply of BIDS molecules in the solution, this method gives a maximal estimate of the number of BIDS molecules bound to the cell that are required to completely

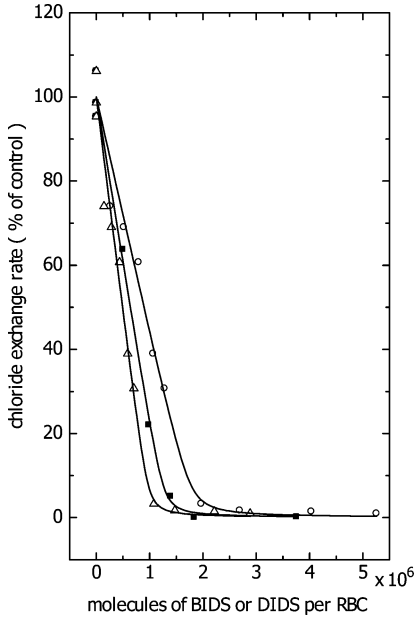

FIGURE 4: Determination of total number of BIDS and DIDS binding sites from the Cl^- exchange inhibition. Red cells were treated with different concentrations of BIDS or DIDS and then washed and loaded with $^{36}Cl^-$ as described in Experimental Procedures. The Cl^- exchange rate constant, expressed as percent of the control rate constant, is plotted as a function of the total number of BIDS or DIDS molecules per RBC present in the original reaction mixture. Data were fitted as described in Experimental Procedures to eq 5, based on the assumption that all BIDS or DIDS molecules present contribute to inhibition of Cl^- exchange. Data for BIDS, with amounts based on weight assuming 100% purity, are shown in open circles; the best fit gives $(1.77 \pm 0.10) \times 10^6$ molecules/cell for 100% inhibition. With BIDS concentration determined by the ϵ value of Rao et al. (62000 M^{-1} cm^{-1}), data (open triangles) correspond to $(0.97 \pm 0.06) \times 10^6$ molecules/cell. For comparison, the DIDS data (solid squares) give $(1.26 \pm 0.07) \times 10^6$ sites/cell.

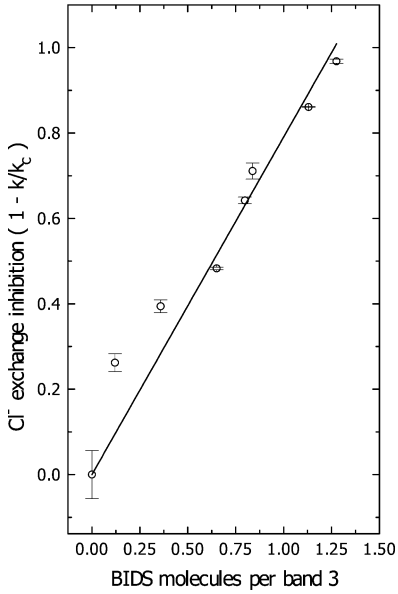

FIGURE 5: Correlation of BIDS binding to RBC membranes and Cl^- exchange inhibition. Cells were treated with 28.6 μM BIDS for various times at pH 8 and 37 °C and washed, and Cl^- exchange rate constants were measured as described in Figure 2. Ghosts were prepared from each cell sample, and the protein concentration was measured by the BCA assay. Ghosts at a concentration of 0.6 mg/mL were solubilized in 0.2% SDS in 5P8, and the optical density was measured at 339 nm, using untreated ghosts at the same concentration as a blank. The concentration of BIDS was calculated using $\epsilon = 51000$ M^{-1} cm^{-1} for BIDS after conjugation to lysine (*21*), and the concentration of band 3 was determined from the protein concentration, assuming that 0.25 of the protein is band 3 with a molecular mass of 101700 Da (*1*). Bars indicate the standard deviation of two flux determinations, except for the control where three measurements were done. The solid straight line is the least squares best fit line, weighting all of the individual data points equally, with the *y*-intercept fixed at zero and a slope of 0.79 ± 0.03, corresponding to 1.27×10^6 sites/cell for complete inhibition.

inhibit Cl^- exchange. This can be compared with the corresponding value for the highest potency disulfonic stilbene inhibitor, DIDS, to see if BIDS has additional binding sites as compared with DIDS.

The results of this experiment are shown in Figure 4. For BIDS (open circles and triangles), as for DIDS (solid squares), the Cl^- exchange activity drops linearly as the number of molecules added increases, until inhibition is nearly complete. Both data sets are fit well with a model based on depletion of the added inhibitor by binding to sites on the red blood cells. In both cases, the apparent dissociation constant for binding is very low and is compatible with measurements of the IC_{50} for reversible inhibition of Cl^- exchange, although the precise value is poorly determined by this type of experiment. Even if we assume that the BIDS is 100% pure and contains no inert material (open circles), the number of binding sites for BIDS is only 40% higher than for DIDS (solid squares). If we adjust the concentration of BIDS by using the extinction coefficient of Rao et al. (*21*) for BIDS ($\epsilon = 62000$ M^{-1} cm^{-1}), there would be slightly fewer sites for BIDS (open triangles) than DIDS. Since DIDS is known to bind very selectively to band 3, this result provides evidence that the great majority of BIDS is also bound to band 3 and that there is not a large population of nonspecific binding sites.

To further examine the selectivity of BIDS for band 3 under our conditions, we labeled intact red cells with 28.6 μM BIDS for various times and plotted the irreversible inhibition of Cl^- exchange, measured after washing away free BIDS with medium containing albumin, against the amount of BIDS bound to membranes from the labeled cells, measured by optical density (Figure 5). Inhibition increases fairly linearly with the amount of BIDS bound, consistent with the hypothesis that both the BIDS and the binding sites are homogeneous in terms of their reaction rate. The amount of BIDS binding associated with complete inhibition of Cl^- exchange is 1.27×10^6 molecules per cell, similar to the number of band 3 molecules per cell, reinforcing the concept that most of the bound BIDS is linked to band 3.

Energy Transfer in Inside-Out Vesicles. Control or BIDS-treated cells were lysed, and ghosts were prepared as described in Experimental Procedures. A portion of each ghost preparation was then treated with 50 μM FM. KI-stripped inside-out vesicles (KIOV's) were prepared from each ghost sample, and some of these were solubilized in SDS and electrophoresed on polyacrylamide gels. Figure 6 shows that more of the FM label was located in band 3 than in any other membrane protein in the KIOV's and that after trypsin cleavage most of this label was found in water-soluble fragments of about 20 kDa, as expected if FM labels Cys-

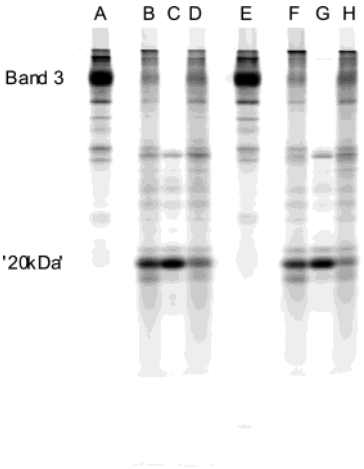

FIGURE 6: Polyacrylamide gel electrophoresis of KIOV's from FM-labeled ghosts. Ghosts and KIOV's were prepared, solubilized in SDS, and electrophoresed as described in Experimental Procedures and Figure 3. Panels A−D show proteins from ghosts that were labeled with 50 μM FM for 30 min at 0 °C in 5P8Cl, as described in Experimental Procedures; panels E−H are similar, except that the ghosts were prepared from cells that were treated with 297 μM BIDS for 60 min at 66% hematocrit, 37 °C, in 150 KH, pH 8, resulting in 97.7% inhibition of Cl^- exchange. Gels were scanned for FM fluorescence on a fluorimager, as described in Experimental Procedures. (A, E) Control; the major labeled band corresponds to the position of band 3 in CB-stained gels (not shown). All other lanes show ghosts that had been treated with 1 μg/mL trypsin at approximately 1 mg/mL ghost protein for 5 min at 0 °C. (B, F) Total ghosts. (C, G) Supernatant after centrifugation (concentrated 1.5×). (D, H) Pellet after centrifugation (concentrated 1.5×). After trypsinization, most of the FM fluorescence is found in a low molecular mass water-soluble fragment, 20 kDa, which probably represents the C-terminal subdomain of the cytoplasmic N-terminal domain of band 3 (*56*) and which contains Cys-201, the probable labeling site, as well as Cys-317.

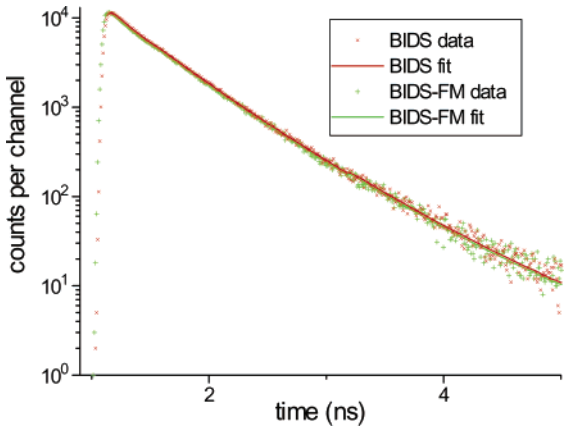

FIGURE 7: Comparison of BIDS fluorescence decay in KIOV's without or with FM labeling. Cells were labeled with BIDS as described in Figure 6. A portion of the ghosts from these cells was labeled with 50 μM FM at 0 °C, as described in Figure 6, and then KIOV's were prepared from both BIDS-labeled and BIDS−FM-labeled ghosts. Single photon counting fluorescence lifetime measurements were performed using a picosecond laser apparatus, as described in Experimental Procedures. For each of these samples, the number of BIDS fluorescence events is plotted against time in nanoseconds. The width of the excitation pulse, including detector response (instrument response function, IRF; not shown), was ~60 ps (fwhm). For these records, the excitation peak occurred at 1.097 ns on the *x*-axis. The data for BIDS-labeled cells are shown as red ×'s, together with a red line representing the best fit of the data to a three-exponential function ($\chi^2 = 1.06$), with τ values of 0.104, 0.410, and 0.714 ns. These values are too close to be resolved accurately, so the lifetime was expressed in terms of the mean τ, $\bar{\tau}$, which was 0.422 ns. A two-exponential fit had a higher χ^2 (1.34), with τ values of 0.193 and 0.537 ns, giving a very similar $\bar{\tau}$ (0.425 ns). The data for BIDS−FM KIOV's, indicated by green +'s, superimpose nearly perfectly on the data for BIDS alone, indicating that there is very little change in the BIDS lifetime because of energy transfer to the FM acceptor. The individual τ values were 0.092, 0.416, and 0.738 ns, and the $\bar{\tau}$ was 0.418 ns.

201 or Cys-317 in the cytoplasmic domain of band 3 (*56*, *57*). Cys-201 is the probable labeling site, because there is evidence that it is more reactive with SH reagents than Cys-317 (*57*). Quantitation of the FM label in the KIOV's by spectrophotometry indicated that total FM labeling was 12.5−13 nmol/mg of ghost protein and that, based on the fraction of FM fluorescence in band 3, there were 0.98−1.02 mol of FM/mol of band 3. This result is like that obtained by Thevenin et al. (*22*) under similar conditions. Thus, as expected if only one SH group (Cys-201) reacts with FM, on average one cytoplasmic SH per band 3 monomer is labeled by FM under these conditions.

Figure 7 shows typical fluorescence decay data for KIOV's from BIDS-labeled cells (points indicated by red ×'s). Surprisingly, the fluorescence decay data fit very poorly to a single exponential decay function. Least squares best fits to a three-exponential function gave χ^2 values that were somewhat smaller (e.g., ranging from 0.83 to 1.59 with mean of 1.20 for the data in Table 1) than those obtained for fits to a two-exponential function (χ^2 values ranging from 1.01 to 2.37 with a mean of 1.71). Attempts to fit to a four-exponential function did not converge. The adequacy of a three-exponential fit (shown by the solid red line in Figure 7) is demonstrated by the fact that plots of the weighted residuals (expressed as a fraction of expected SD) did not show a systematic deviation with increasing time (e.g., red line in Figure 8) and most of the residuals were less than 2 times the expected SD. The three-exponential decay behavior of BIDS might reflect either intrinsic characteristics of the BIDS molecule, such as rotational isomers, or heterogeneity in the environment around different populations of BIDS molecules in BIDS-labeled red cells. When BIDS was conjugated to lysine and suspended in acetonitrile (to provide a less polar environment, where BIDS decay rate would be less rapid than in water and more similar to that in labeled membranes), the data (not shown) also were best fit with three exponentials ($\chi^2 = 1.08$ compared with 3.68 for two-exponential fit). Thus it seems likely that the complexity in the BIDS fluorescence decay represents an intrinsic characteristic of BIDS. Multiple lifetimes have also been observed for tryptophan (*58*) as well as for single molecule fluorescence (*59*), where there is no possibility of heterogeneity in labeling sites.

Figure 7 also shows fluorescence decay data for KIOV's from BIDS-labeled cells which had been made into ghosts and then labeled with 50 μM FM before KIOV's were prepared (points indicated by green +'s). The data superimpose nearly perfectly over those without FM labeling (red ×'s). This becomes even clearer from the residual plots in Figure 8, where the green line shows the weighted residuals for the difference between the data for ghosts labeled with BIDS alone compared to the decay curve calculated from data for BIDS−FM-labeled ghosts (scaled to give matching peak intensities), while the red line shows the comparison of the data for BIDS−FM ghosts to the fitted BIDS−FM

Table 1: Energy Transfer Efficiency for BIDS−FM_i-Labeled AE1 in Ghosts or KIOV's[a]

		BID					BIDS + FM					
	BIDS	2-exp		3-exp		FM	2-exp		3-exp		*E* (%)	
expt	label	χ^2	$\bar{\tau}$	χ^2	$\bar{\tau}$	label	χ^2	$\bar{\tau}$	χ^2	$\bar{\tau}$	2-exp	3-exp
1	A	1.95	0.394	1.13	0.395	T	1.68	0.401	1.13	0.395	−1.8	0.0
2	B	1.34−1.66	0.420 ± 0.008	1.06−1.11	0.419 ± 0.007	T	1.35−1.41	0.417 ± 0.005	1.04−1.24	0.415 ± 0.005	0.8	1.0
3	E60	2.37	0.393	1.59	0.399	T	2.37−2.94	0.375 ± 0.004	1.67−1.84	0.392 ± 0.001	4.7	1.9
4a	E10	2.17−2.17	0.288 ± 0.002	1.44−1.47	0.300 ± 0.005	R	2.62−2.84	0.276 ± 0.011	1.57−1.76	0.288 ± 0.017	4.2	4.2
4b						T	2.41	0.282	1.58	0.294	2.1	2.0
4c	E60	2.02	0.297	1.48	0.292	R2	1.89	0.296	1.49	0.298	0.3	−2.1
4d						R	2.04	0.269	1.45	0.268	9.4	8.2
4e	C	1.94	0.310	1.34	0.307	R1.5	2.03	0.300	1.53	0.298	3.2	2.9
4f						T	1.93	0.299	1.51	0.297	3.5	3.3
5a	D	1.01	0.279	0.83	0.277	T	1.02	0.271	0.83	0.268	2.9	3.2
5b	D′	1.16	0.255	0.95	0.252	T	1.14	0.248	0.91	0.246	2.7	2.4
5c	D*	1.10	0.283	0.89	0.277	T	1.05	0.271	0.91	0.268	4.2	3.2
mean			0.324		0.324			0.309		0.311	3.0	2.5
SEM			0.020		0.021			0.016		0.016	0.8	0.7
N			9		9			12		12	12	12

[a] BIDS labeling conditions: A, 40 μM BIDS, 44% hct, 37 °C, 30 min; B, 297 μM BIDS, 44% hct, 37 °C, 60 min; C, 200 μM BIDS, 44% hct, 37 °C, 1.5 h; D, 24 μM BIDS, 25% hct, 37 °C, 30 min; D′, 53 μM BIDS, 25% hct, 37 °C, 1.5 h; D*, cells were preincubated with 400 μM DNDS before labeling as in D; E, the method of Rao et al. (*21*) with 60 or 10 min reaction time at 37 °C, 205 μM BIDS, 44% hct. FM labeling conditions: T, the method of Thevenin et al. (*22*) (50 μM FM, 0 °C, 30 min); R, the method of Rao et al. (*21*) (1 mM FM, 37 °C, 1 h); R1.5 and R2 indicate labeling for 1.5 or 2 h, respectively. Errors, when shown, represent SEM of two or three replicates. KIOV's were used in experiment 2.

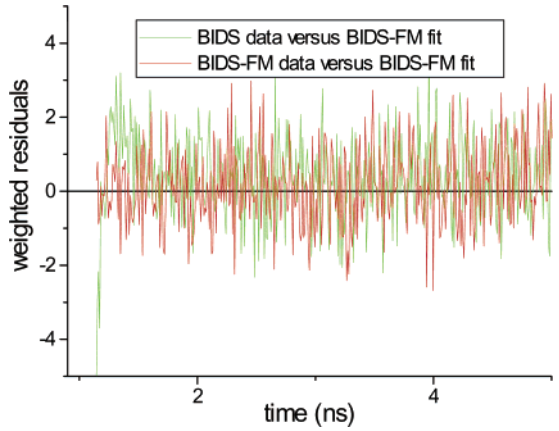

FIGURE 8: Residual plot of BIDS fluorescence decay. Deviations of the data from the best fit are expressed as weighted residuals (p 121 of ref *48*)—actual value minus value calculated from best fit divided by the square root of the calculated number of counts (expected standard deviation, SD)—and are plotted as a function of time. The red line shows the residuals for the fit of a three-exponential function to the data for BIDS−FM KIOV's shown in Figure 7. The green line represents the residuals calculated by using the data points for KIOV's from cells labeled with BIDS alone (red ×'s in Figure 7), together with the best fit three-exponential function for the BIDS−FM data. (The BIDS data were scaled by a factor of 0.972, determined from the ratio of data for BIDS and BIDS−FM for the first 0.19 ns, to correct for the slightly higher peak fluorescence values for the BIDS data set.) These residuals are of the same magnitude as those for the actual BIDS−FM data to which the function was fitted. This, as well as the lack of a significant trend in the residuals with time, demonstrates that there is very little difference in the decay rate of BIDS fluorescence with or without FM labeling.

decay curve. Note that the fit of the BIDS-alone data to the BIDS−FM decay curve is nearly as good as that of the BIDS−FM data, and there is no systematic deviation as a function of time, as would be expected if the two data sets had different fluorescence decay rates.

Although a three-exponential function provided the best fit to the data, the lifetimes of the three components differed by less than a factor of 10. In cases such as this, because of the mathematical difficulties in fitting multiple exponential functions, the individual τ values are not very well determined. Because there is no evidence to indicate that the various τ values represent distinct populations of BIDS, the best measure of the time dependence of BIDS fluorescence is given by the average lifetime, $\bar{\tau}$, defined as described in Experimental Procedures (*49*). The average of three values of $\bar{\tau}$ determined from three-exponential fits to data for KIOV's from BIDS-labeled cells was 0.419 ± 0.007 ns. When the ghosts from the BIDS-labeled cells were treated with FM, the corresponding mean of three determinations of $\bar{\tau}$ was 0.415 ± 0.005 ns, giving a calculated energy transfer of 1.0%. Data with two-exponential fits gave similar $\bar{\tau}$ values, with energy transfer of 0.8%.

These results are very different from those expected on the basis of the energy transfer data presented by Rao et al. (*21*). From their energy transfer values of 46−47%, one would expect the BIDS lifetime for the FM-treated KIOV's to be only 53−54% of the lifetime for the KIOV's with BIDS alone, a difference that would easily be resolved with the present instrumentation. The data in Figure 7 thus indicate that the BIDS and FM labeling sites are much farther apart than indicated by the earlier data (*21*).

Energy Transfer in Ghosts Using Various Labeling Conditions. Because our results differed so strikingly from those of Rao et al. (*21*), and because their experiments were done with red cell ghosts, rather than KIOV's, we repeated the labeling and fluorescence lifetime measurements in red cell ghosts. Table 1 shows the results from a series of experiments in which the BIDS labeling conditions were varied and the FM labeling was done either at 50 μM, as in our experiments and those of Thevenin et al. (*22*), or at 1 mM as in the experiments of Rao et al. (*21*). Figure 9 shows the FM fluorescence in SDS−polyacrylamide gels of the FM-labeled ghosts. As expected, because the ghosts contain much larger quantities of peripheral proteins, such as spectrin, attached to the inner surface of the membrane, the FM labeling in

FIGURE 9: Polyacrylamide gel electrophoresis of FM-labeled ghosts. Cells were divided into two portions, one of which was treated with 205 μM BIDS at 44% hematocrit, 37 °C, pH 8, for 10 min (lanes A and B) and the other of which was treated for 60 min (lanes C and D). The former treatment gave 60% inhibition of anion exchange, while the latter caused 97% inhibition. Ghosts were prepared and labeled with FM, either 1 mM at 37 °C, pH 7.4, for 60 min in 5P7.4 (lanes A and C) or 50 μM at 0 °C, pH 8, for 30 min (lanes B and D) in 5P8 supplemented with 135 mM NaCl and 0.1 mM EDTA (5P8Cl). In the latter condition, 0.2 mM dithiothreitol was added at the end of the reaction time to quench the reaction. Ghosts were solubilized in SDS and electrophoresed on 12% polyacrylamide gels, and fluorescence was visualized on a fluorimager, as described in Experimental Procedures. In each case the major FM-labeled band corresponded to band 3. The labeling pattern was similar at the high and low FM concentration, except that additional labeling of bands other than band 3, particularly band 4.1, was seen at the higher FM concentration (lanes A and C).

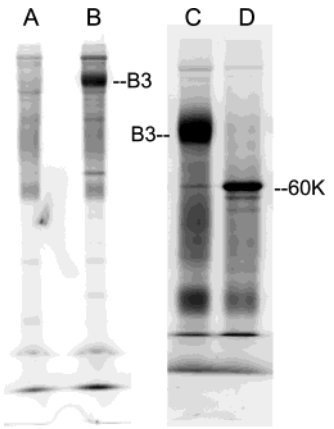

FIGURE 10: Labeling of intact red blood cells with BIDS and external FM (FM_o). Cells were labeled with 212 μM BIDS and/or with 1 mM FM as described in Experimental Procedures. After being washed to remove free FM, the cells were either made into ghosts or cleaved by chymotrypsin and then made into ghosts. Ghosts were solubilized in SDS and electrophoresed in 12% (A, B) or 9% (C, D) polyacrylamide gels, and fluorescence was imaged as described in Experimental Procedures. Lanes: A, ghosts from FM-labeled, BIDS-blocked cells; B, no BIDS treatment; C, ghosts from FM-labeled cells; lane D, the external chymotryptic cleavage product of (C).

ghosts is much less specific for band 3 than it is when KIOV's are prepared (compare with Figure 6), and this is particularly true at the higher FM concentrations (lanes A and C). The total FM labeling rose from 13.1 to 15.5 nmol/mg of protein with 50 μM FM to 29−30 nmol/mg of protein with 1 mM FM; the corresponding labeling in the band 3 region of gels was 2.4−4.8 and 11.8−12 mol/mol of band 3, respectively. For comparison, Rao et al. (*21*) reported 8.2 nmol/mg of protein for ghosts (about 3.3 mol/mol of band 3) and 18−22 nmol/mg of purified band 3 (1.8−2.2 mol/mol of band 3). FM labeling under our reaction conditions was at least as large as in the experiments of Rao et al., so any lack of energy transfer in our experiments could not be ascribed to a failure of the acceptor (FM) to react with band 3.

Table 1 shows the average lifetimes calculated from two- or three-exponential fits to the data for ghosts or KIOV's (experiment 2). In all cases the $\bar{\tau}$ values without or with FM treatment were very similar, indicating that E was very small, regardless of the method used to label with BIDS or FM. Even when DNDS was used to reduce the amount of BIDS binding to AE1 (D*), and thus reveal any effects of nonspecific labeling by BIDS, the results were similar. The average energy transfer from the three-exponential data was 2.5 ± 0.7% (SEM, N = 12) and for the two-exponential data was 3.0 ± 0.8%. The highest energy transfer values were found when the methods of Rao et al. were used to label with BIDS and FM, perhaps because the higher concentrations, times, and temperatures used could have caused labeling of additional sites, but energy transfer values as high as those reported earlier were never observed. If only the three-exponential data with 0 °C 50 μM FM labeling were used, which should have the best labeling specificity and which exhibited the best χ^2 values, the energy transfer percentage was 2.1 ± 0.4%.

Contributions of External FM Labeling to Fluorescence Energy Transfer. A possible explanation for the higher energy transfer seen in some experiments where we used the labeling methods of Rao et al. could be that there is an additional FM labeling site at Lys-430, an externally accessible site that is labeled by eosin-5-maleimide (EM) (*60*). Indeed, Bicknese et al. (*41*) have shown that, at 1 mM, FM does label a site in intact red cells which is probably Lys-430. Macara and Cantley (*30*) showed that if red blood cells are labeled with substoichiometric amounts of BIDS (far less than required to saturate the band 3 sites) and then with EM, substantial energy transfer (14−31%) is observed from BIDS to EM, so it is likely that BIDS might transfer some energy to FM located at this site. When we labeled intact red cells with FM under the conditions of Rao et al. and visualized the labeled proteins by SDS−PAGE, there was substantial labeling of band 3 and of the 60K chymotryptic fragment of band 3 (Figure 10, lanes B−D), demonstrating that external FM can label a site in the 60K segment, probably Lys-430, under the conditions of Rao et al. Pretreatment with BIDS prevented this labeling (lane A), demonstrating that FM at Lys-430 could not serve as an *intra*molecular acceptor for energy transfer from BIDS. Because the extent of BIDS

labeling of AE1 was probably over 80% in the experiments of Rao et al., few sites would be available for external FM labeling, so the contribution of this additional acceptor is probably insufficient to explain the larger energy transfer they observed.

Determination of the Critical Transfer Distance, R_0. To check the value of R_0 given by Rao et al., we measured the quantum yield of BIDS in ghosts from BIDS-labeled cells, as described in Experimental Procedures, and obtained a quantum yield of 0.088, somewhat lower than their value of 0.16. To determine the overlap integral, *J*, we multiplied the normalized fluorescence of BIDS-labeled ghosts by the extinction coefficient for FM-labeled ghosts over the same part of the spectrum, using 1 nm intervals. Assuming $\kappa^2 = {}^2/_3$ (*45*, *46*), the value for random orientation of donor and acceptor dipoles, and taking the refractive index as 1.34, we obtained an R_0 value (*50*) of 36.04 Å, slightly higher than the value of 34.6 Å reported by Rao et al. (*21*).

Steady-State Fluorescence Measurements. The measurements (*21*) of energy transfer in red cell ghosts by Rao et al. were done by steady-state donor quenching or sensitized emission of the acceptor, whereas we measured donor fluorescence decay. To see whether the difference in methods might account for the different results, we performed steady-state fluorescence measurements on ghosts from cells labeled with external BIDS, with internal FM, or with both external BIDS and internal FM.

Figure 11A shows the emission spectra for these three types of ghosts, with excitation at 334 nm, near the maximum for BIDS. In all cases, the spectra for control ghosts have been subtracted. The dotted line [visible only at the right, superimposes over the dash−dot (uppermost) line at the left] shows the spectrum for BIDS-labeled ghosts, which have the expected emission peak around 425 nm. In comparison, the ghosts with both BIDS and FM labeling (solid line) show some decrease in fluorescence around 425 nm and a very large peak around 520 nm, where fluorescein emission is expected. In this and other measurements, including an experiment with KIOV's, the apparent quenching around 425 nm was always ≤8%. Even this minor quenching, however, is nearly entirely accounted for by the additional optical density at the excitation and emission wavelengths resulting from FM treatment, reducing the value of *E* calculated from all donor quenching experiments to ≤3%. The dashed line (visible only at the left, superimposes over the solid line at the right) shows the spectrum for ghosts labeled only with FM. From this it is apparent that the entire increase in fluorescence around 520 nm is actually due to direct excitation of the acceptor (FM). The sum of the emission for ghosts labeled separately with either FM or BIDS (dash−dot line) in the 500−560 nm region is indistinguishable from that for the ghosts labeled with both BIDS and FM. Similar results (not shown) were obtained with KIOV's. Thus, there is no evidence for significant sensitized emission or donor quenching resulting from energy transfer.

Although the excitation wavelength for the energy transfer experiments is not stated in Table 2 of Rao et al., where the energy transfer data are presented, it appears from other experiments described in the paper that 350 nm may have been used. On p 4509 of their paper, Rao et al. state: "Since the excitation peaks and the emission peaks of this donor−acceptor pair (BIDS and FM) are well separated, there was

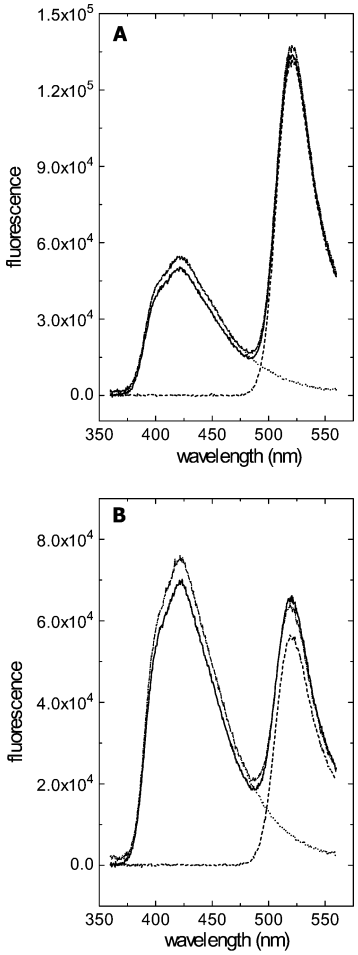

FIGURE 11: Fluorescence emission spectra of ghosts from FM, BIDS, and FM + BIDS-labeled cells with excitation at 334 nm (A) or 350 nm (B). Cells at 25% hct in 150KH, pH 8, were labeled with 21.2 μM BIDS for 60 min. Ghosts were prepared in 5P8, and some of these ghosts as well as control ghosts were labeled with 50 μM FM by incubation at 0 °C for 30 min as described in Experimental Procedures. The ghosts were suspended at 0.2 mg/mL, and corrected emission spectra were measured. All spectra have the spectrum for unlabeled ghosts subtracted. Key: solid line, BIDS−FM labeled; dashed line, FM labeled; dotted line, BIDS labeled; dash−dot line, sum of curves for FM-labeled and BIDS-labeled ghosts.

essentially no background correction and the error in the [sensitized emission] measurement was less than 10%." To see whether this may have been true with excitation at 350 nm, even though it was clearly not so with 334 nm excitation, we repeated the experiments at 350 nm (Figure 11B). This indeed reduced the contribution of direct FM excitation to the apparent sensitized emission peak, but as in Figure 11A, the sum of the BIDS and FM emissions at 520 nm was approximately equal to that observed for the doubly labeled ghosts, providing no evidence for significant sensitized emission.

It seems very likely that a similar problem may have affected the measurements of Rao et al., because their FM labeling stoichiometry (8.2 nmol/mg of protein) was not much smaller than ours (13.3 nmol/mg). Besides the very large FM background, there is an additional contribution to the fluorescence at 520 nm due to the small but significant fluorescence of BIDS-labeled ghosts at this wavelength (dotted lines in Figure 11). In Figure 2C of their paper, Rao et al. also report considerable BIDS fluorescence at 520 nm.

In view of these observations, it is difficult to understand how they could measure sensitized emission with essentially no background corrections. Had we ignored the background corrections, we would have thought that there was very large energy transfer from BIDS to FM, like that which they reported. Thus, our data suggest a reasonable explanation for their energy transfer values measured by sensitized emission.

Our steady-state data, however, provide no clear explanation for the observation of Rao et al. of similar energy transfer by donor quenching. If no corrections were made for the inner filter effect, our data would indicate some donor quenching, but not the amount that would give an *E* value of 46% as they reported. Also, they report using triangular cuvettes, which should reduce inner filter effects. The explanation of their donor quenching observations thus remains a mystery, but it is clear that we cannot replicate their observations. Our steady-state measurements give results consistent with the fluorescence decay observations, namely, very little energy transfer from BIDS to FM at the inner SH sites.

DISCUSSION

Estimate of Distance between Cys-201 and the BIDS Site. From eq 10 and the mean energy transfer percent determined from all of the three-exponential data fits in Table 1, the BIDS−FM distance is 63.6 Å using the value of 34.6 Å for R_0 (*21*) or 66.3 Å using our value of 36.0 Å for R_0. Addition of 1 SE to the *E* values gives distances of 61 and 63.5 Å, respectively. The value of 3% energy transfer from the steady-state data gives distances of 61.8 and 64.3 Å. If we take 40 Å as the distance between FM bound to Cys-201 and the lipid headgroups at the cytoplasmic side of the membrane bilayer (*61*), then these data would place BIDS 21.8−26.3 Å from the cytoplasmic surface of the membrane, that is, somewhere near the middle of the lipid bilayer (see magenta rectangles in Figure 1), assuming a membrane thickness of about 45 Å (*21*). Because the mean energy transfer is so small, and because little or no energy transfer was seen under the most specific labeling conditions (KIOV's, Figure 7), the possibility that BIDS is located farther toward the external side of the membrane cannot be excluded.

This distance estimate is based on the assumption that $\kappa^2 = {}^2/_3$, which strictly only applies to the case where donor and acceptor transition dipoles are randomly oriented (*45*, *46*). Although depolarization data indicate that BIDS is probably rigidly fixed in the band 3 structure (*21*), FM at the cytoplasmic cysteine site exhibits two components of fluorescence depolarization (*56*). The more rapid component, with $\tau \leq 150$ ps, exhibits residual anisotropy that can be modeled as corresponding to random motion within a cone of 44° semiangle (*22*, *56*). Hillel and Wu (*51*) performed Monte Carlo calculations of the effect of uncertainty in κ^2 on the donor−acceptor distance, for the case where one transition moment is fixed and the other is free to reorient on the surface of a cone of 35° semiangle. Based on a value of 3.0% for *E*, with $R_0 = 36.0$, the peak of the probability density is located at 62.5 Å, with a lower limit of 49 Å and an upper limit of 80.4 Å. If the membrane thickness is taken as 45 Å, and 40 Å is subtracted for the distance from the FM site to the inner surface of the membrane (*22*), the most probable value would place the BIDS site near the center of the bilayer. Even the extreme limits, which have a very low probability and are based on a model with more restricted motion than was observed for FM (35° semiangle cone rather than 44°), demonstrate that BIDS must be at least 9 Å from the inner surface of the membrane.

Comparison with Previous Data. Our data, like those of Thevenin et al. (*22*), were obtained entirely with ghosts or KIOV's, where the band 3 conformation is unlikely to be greatly altered from that in intact red blood cells. In contrast, most of the data reported by Rao et al. (*21*), including all of the data with donor−acceptor pairs other than BIDS−FM, were obtained with purified band 3 solubilized in Triton X-100, where the possibity of changes in the protein structure is more likely. The only data in ghosts reported by Rao et al. are two measurements with BIDS−FM, one by donor quenching and the other by stimulated emission, and the latter probably overestimates *E* because of failure to correct for background fluorescence, as described above. The fact that these two measurements agreed well with a single stimulated emission measurement with BIDS−FM in purified band 3, as well as with a donor quenching and lifetime measurement for BIDS with NBD (4-nitrobenz-2-oxa-1,3-diazole) used as acceptor, was taken as evidence that the band 3 structure was unaltered in the purified, detergent-solubilized band 3. In view of the questions raised about the steady-state experiments in ghosts, this evidence is weak at best. Although the disulfonic stilbene site seems to retain its high affinity in suitable nonionic detergents (*43*), recent crystallographic evidence combined with earlier cross-linking data indicates that the cytoplasmic domain of band 3 can undergo conformational changes that result in considerable displacements of Cys-201 and Cys-317 (*62*, *63*). This possibility is supported by data demonstrating pH-dependent changes in segmental motional freedom of parts of the band 3 cytoplasmic domain (*56*). Thus, it seems likely that conformational changes in detergent may have contributed to the energy transfer observed by Rao et al. in purified band 3.

Rao et al. determined the fluorescence lifetime of BIDS by a modulation technique using frequencies of 30 and 18 MHz, and a single lifetime of 0.81 ns is reported, probably from data with purified band 3. In contrast, our BIDS decay data required a three-exponential fit and gave a much shorter average lifetime, with a $\bar{\tau}$ value of 0.32 ± 0.02 ns (Table 1). Rao et al. state that "99% of the BIDS fluorescence intensity exhibited a single-exponential decay", but the apparent basis for this statement is agreement between the lifetimes as determined by phase shift (τ_φ) and by demodulation (τ_m). Even at the highest frequency used, however, the phase shift corresponding to 0.81 ns would only be 8.7° and the demodulation (decrease in intensity of the fluctuating signal) would be only 1.2% (*50*), that is, a decrease from 100% to 98.8%. The possibility of inaccuracy in the latter value casts doubt on the evidence for a monoexponential decay.

As mentioned above, our steady-state measurements indicate that failure to correct for the background fluorescence of FM might explain the high *E* value obtained by Rao et al. from sensitized emission. The reason for their observation of 46% donor quenching is not clear, although both our lifetime and donor fluorescence data indicate far less quenching, ≤3%. Besides the two measurements in ghosts, Rao et al. provide 12 other measurements of *E* in

detergent-solubilized, purified band 3, with BIDS and FM or other donor−acceptor pairs, which agree fairly well with their results for ghosts. In all of these cases, however, either the donor or acceptor labels more than one site on band 3, and in many cases the values of E are ≤ 0.2. This, together with the possibility of changes in band 3 structure upon detergent solublization, casts doubt on the degree to which these data corroborate the results in ghosts.

Implications of a Longer Distance between BIDS and the FM-Labeled Cytoplasmic SH. Our data, unlike those of Rao et al., do not constrain the disulfonic stilbene (BIDS) site to be located near the cytoplasmic side of the membrane. Instead, the site is probably located near the middle or even in the external half of the membrane (shown by solid magenta rectangles in Figure 1).

Such a location would be more compatible with evidence that the disulfonic stilbene H_2DIDS can react with Lys-539 and Lys-851 (*23*), both of which are thought to lie near the external side of the membrane (*4*, *24*, *25*, *28*, *29*). It would also fit with NMR evidence that reaction of Glu-681 with Woodward's reagent K, a carboxylic acid reagent that forms a large, negatively charged adduct, does not prevent external DIDS binding (*64*). On the basis of substituted cysteine accessibility measurements, Glu-681 is probably located in an α-helix three amino acids from the cytoplasmic side of the apolar portion of the bilayer (*65*), which would place it about 5−7 Å from the inner surface of the membrane (orange circles in Figure 1). If the disulfonic stilbene site were also near the cytoplasmic side (as indicated by the crosshatched magenta rectangle in Figure 1), assuming that it is in the same polar access channel as Glu-681, Woodward's reagent K would be expected to block DIDS binding, but it does not. Furthermore, evidence from Jennings and Anderson (*66*) that prior H_2DIDS reaction prevents WRK reaction with Glu-681 suggests that the DS site is farther toward the outside of the membrane than is the Glu-681 site, again compatible with our measurements placing the BIDS site (probably near to or identical with the H_2DIDS site) approximately 23 Å (as indicated by the solid magenta rectangles in Figure 1) or even farther from the membrane cytoplasmic surface.

The fact that Glu-681 may participate in gating of protons across the band 3 permeability barrier during band 3-mediated proton−sulfate transport (*67*−*69*) and that modification of this residue affects anion selectivity (*70*), together with evidence that disulfonic stilbene binding is very strongly affected by the orientation of the Cl^- transport site (with much higher affinity for the outward-facing form) (*20*), indicates that both Glu-681 and the DS site are involved in the ion translocation process. Thus, the transport mechanism of band 3 must involve coordinated conformational changes in parts of the protein that are separated by about 15 Å or more, rather than a very localized conformational change in a small region of the protein near the cytoplasmic membrane surface, as suggested by the previous BIDS−FM distance determination. Binding of DNDS, another DS, causes changes in the accessibility to biotin maleimide of a number of sites that are accessible from the external side of the membrane, providing further evidence for widespread conformational changes in AE1 (*71*). The concept of a more "global" conformational change during transport is supported by the large activation volume displayed by band 3-mediated sulfate transport (*72*) and by the effects of transport site conformation on the affinities of various inhibitors (*40*). On the basis of the high-resolution crystal structure of a bacterial (*Escherichia coli*) anion exchanger, GlpT, a "rocker switch" mechanism has been proposed (*31*), in which an aqueous cavity inside the protein, containing an anion binding site composed of positively charged arginines, becomes alternately accessible to the cytoplasmic or periplasmic side of the *E. coli* membrane. The access of the inner cavity to one side or the other is controlled by two gates, located over 20 Å apart, that open and close by random thermal oscillations between different protein conformational states and that are structured so that one gate closes when the other is opened. Another recent crystal structure of the mitochondrial ATP−ADP exchanger suggests a similar gated cavity mechanism (*32*). Our evidence for separation of the BIDS and Glu-681 sites would be compatible with such a mechanism, although other mechanisms, such as rotation of transmembrane helices (*73*, *74*), that cause coordinated changes in structure at various distances from the cytoplasmic membrane surface, cannot be ruled out. Further examination of these proposed large-scale conformational changes during the transport cycle in AE1, by means of FRET and other techniques, should provide more detailed information on the molecular mechanism that transports ions in this and other coupled transport systems.

ACKNOWLEDGMENT

The authors thank Monica Carmichael, Shawn Lucas, and Mark Wilson for assistance in the early stages of this work, Dr. Xiuzhi Wang for synthesis of BIDS, Cheryl Wu, Dipesh Risal, and Prithwish Pal for assistance with some of the experiments presented, Alvin Law for help in preparation of some of the illustrations, and Dr. Chris Collison for helpful suggestions concerning the manuscript.

REFERENCES

1. Lux, S. E., John, K. M., Kopito, R. R., and Lodish, H. F. (1989) Cloning and characterization of band 3, the human erythrocyte anion-exchange protein (AE1), *Proc. Natl. Acad. Sci. U.S.A. 86*, 9089−9093.
2. Jennings, M. L. (1992) Cellular anion transport, in *The Kidney: Physiology and Pathophysiology* (Seldin, D. W., and Giebisch, G., Eds.) pp 113−145, Raven Press, New York.
3. Knauf, P. A. (1989) Kinetics of anion transport, in *The Red Cell Membrane* (Raess, B. U., and Tunnicliff, G., Eds.) pp 171−200, Humana Press, Clifton, NJ.
4. Knauf, P. A., and Pal, P. (2003) Band 3 mediated transport, in *Red Cell Membrane Transport in Health and Disease* (Bernhardt, I., and Ellory, J. C., Eds.) pp 253−301, Springer, Berlin.
5. Passow, H. (1986) Molecular aspects of band 3 protein-mediated anion transport across the red blood cell membrane, *Rev. Physiol. Biochem. Pharmacol. 103*, 61−223.
6. Alper, S. L. (1991) The band 3-related anion exchanger (AE) gene family, *Annu. Rev. Physiol. 53*, 549−564.
7. Jennings, M. L. (1992) Anion transport proteins, in *The Kidney: Physiology and Pathophysiology* (Seldin, D. W., and Giebisch, G., Eds.) pp 503−535, Raven Press, New York.
8. Simon, J. S., Deshmukh, G., Couch, F. J., Merajver, S. D., Weber, B. L., Van Vooren, P., Tissil, F., Szpirer, J., Szpirer, C., Alper, S. L., Jacob, H. J., and Brosius, F. C., III (1996) Chromosomal mapping of the rat Slc4a family of anion exchanger genes, Ae1, Ae2, and Ae3, *Mamm. Genome 7*, 380−382.
9. Wang, D. N., Sarabia, V. E., Reithmeier, R. A. F., and Kuhlbrandt, W. (1994) Three-dimensional map of the dimeric membrane domain of the human erythrocyte anion exchanger, band 3, *EMBO J. 13*, 3230−3235.

10. Kampmann, L., Lepke, S., Fasold, H., Fritzsch, G., and Passow, H. (1982) The kinetics of intramolecular cross-linking of the band 3 protein in the red blood cell membrane by 4,4′-diisothiocyanodihydrostilbene-2,2′-disulfonic acid (H_2DIDS), *J. Membr. Biol. 70*, 199−216.
11. Rakitzis, E. T., Gilligan, P. J., and Hoffman, J. F. (1978) Kinetic analysis of the inhibtion of sulfate transport in human red blood cells by isothiocyanates, *J. Membr. Biol. 41*, 101−115.
12. Shami, Y., Rothstein, A., and Knauf, P. A. (1978) Identification of the Cl^- transport site of human red blood cells by a kinetic analysis of the inhibitory effects of a chemical probe, *Biochim. Biophys. Acta 508*, 357−363.
13. Wood, P. G., Müller, H., Sovak, M., and Passow, H. (1992) Role of Lys 558 and Lys 869 in substrate and inhibitor binding to the murine band 3 protein: a study of the effects of site-directed mutagenesis of the band 3 protein expressed in the oocytes of *Xenopus laevis*, *J. Membr. Biol. 127*, 139−148.
14. Aranibar, N., Ostermeier, C., Legrum, B., Rüterjans, H., and Passow, H. (1994) Influence of stilbene disulfonates on the accessibility of the substrate-binding site for anions in the band 3 protein (AEB1), *Renal Physiol. Biochem. 17*, 187−189.
15. Salhany, J. M., Sloan, R. L., Cordes, K. A., and Schopfer, L. M. (1994) Kinetic evidence for ternary complex formation and allosteric interactions in chloride and stilbenedisulfonate binding to band 3, *Biochemistry 33*, 11909−11916.
16. Knauf, P. A., Ries, E. A., Romanow, L. A., Bahar, S., and Szekeres, E. S. (1993) DNDS (4,4′-dinitrostilbene-2,2′-disulfonate) does not act as a purely competitive inhibitor of red blood cell band 3-mediated anion exchange, *Biophys. J. 64*, A307.
17. Falke, J. J., and Chan, S. I. (1986) Molecular mechanisms of band 3 inhibitors. 1. Transport site inhibitors, *Biochemistry 25*, 7888−7894.
18. Kaplan, J. H., Scorah, K., Fasold, H., and Passow, H. (1976) Sidedness of the inhibitory action of disulfonic acids on chloride equilibrium exchange and net transport across the human erythrocyte membrane, *FEBS Lett. 62*, 182−185.
19. Fröhlich, O. (1982) The external anion binding site of the human erythrocyte anion transporter: DNDS binding and competition with chloride, *J. Membr. Biol. 65*, 111−123.
20. Furuya, W., Tarshis, T., Law, F.-Y., and Knauf, P. A. (1984) Transmembrane effects of intracellular chloride on the inhibitory potency of extracellular H_2DIDS. Evidence for two conformations of the transport site of the human erythrocyte anion exchange protein, *J. Gen. Physiol. 83*, 657−681.
21. Rao, A., Martin, P., Reithmeier, R. A. F., and Cantley, L. C. (1979) Location of the stilbene disulfonate binding site of the human erythrocyte anion-exchange system by resonance energy transfer, *Biochemistry 18*, 4505−4516.
22. Thevenin, B. J., Bicknese, S. E., Verkman, A. S., and Shohet, S. B. (1996) Distance between Cys-201 in erythrocyte band 3 and the bilayer measured by single-photon radioluminescence, *Biophys. J. 71*, 2645−2655.
23. Okubo, K., Kang, D., Hamasaki, N., and Jennings, M. L. (1994) Red blood cell band 3: lysine 539 and lysine 851 react with the same H_2DIDS (4,4′-diisothiocyanodihydrostilbene-2,2′-disulfonic acid) molecule, *J. Biol. Chem. 269*, 1918−1926.
24. Zhu, Q., Lee, D. W., and Casey, J. R. (2003) Novel topology in C-terminal region of the human plasma membrane anion exchanger, AE1, *J. Biol. Chem. 278*, 3112−3120.
25. Zhu, Q., and Casey, J. R. (2004) The substrate anion selectivity filter in the human erythrocyte Cl-/HCO3 exchange protein, AE1, *J. Biol. Chem. 279*, 23565−23573.
26. Jarolim, P., Murray, J. L., Rubin, H. L., Smart, E., and Moulds, J. M. (1997) Blood group antigens Rb(a), Tr(a), and Wd(a) are located in the third ectoplasmic loop of erythroid band 3, *Transfusion 37*, 607−615.
27. Jarolim, P., Murray, J. L., Rubin, H. L., Coghlan, G., and Zelinski, T. (1997) A Thr552 → Ile substitution in erythroid band 3 gives rise to the Warrior blood group antigen, *Transfusion 37*, 398−405.
28. Fujinaga, J., Tang, X.-B., and Casey, J. R. (1999) Topology of the membrane domain of human erythrocyte anion exchange protein, AE1, *J. Biol. Chem. 274*, 6626−6633.
29. Popov, M., Li, J., and Reithmeier, R. A. F. (1999) Transmembrane folding of the human erythrocyte anion exchanger (AE1, band 3) determined by scanning and insertional N-glycosylation mutagenesis, *Biochem. J. 339*, 269−279.
30. Macara, I. G., and Cantley, L. C. (1981) Interactions between transport inhibitors at the anion binding sites of the band 3 dimer, *Biochemistry 20*, 5095−5105.
31. Huang, Y., Lemieux, M. J., Song, J., Auer, M., and Wang, D. N. (2003) Structure and mechanism of the glycerol-3-phosphate transporter from *Escherichia coli*, *Science 301*, 616−620.
32. Pebay-Peyroula, E., Dahout-Gonzalez, C., Kahn, R., Trezeguet, V., Lauquin, G. J., and Brandolin, G. (2003) Structure of mitochondrial ADP/ATP carrier in complex with carboxyatractyloside, *Nature 426*, 39−44.
33. Knauf, P. A., Law, F.-Y., and Atherton, S. J. (1999) Relocation of the disulfonic stilbene (DS) sites of band 3 (AE1) on the basis of fluorescence lifetime measurements, *Biophys. J. 76*, A233.
34. Steck, T. L., and Kant, J. A. (1974) Preparation of impermeable ghosts and inside-out vesicles from human erythrocyte membranes, *Methods Enzymol. 31*, 172−180.
35. Bennett, V. (1983) Proteins involved in membrane-cytoskeleton association in human erythrocytes: spectrin, ankyrin, and band 3, *Methods Enzymol. 96*, 313−324.
36. Jennings, M. L., and Nicknish, J. S. (1984) Erythrocyte band 3 protein: evidence for multiple membrane-crossing segments in the 17 000-dalton chymotryptic fragment, *Biochemistry 23*, 6432−6436.
37. Kotaki, A., Naoi, M., and Yagi, K. (1971) A diaminostilbene dye as a hydrophobic probe for proteins, *Biochim. Biophys. Acta 229*, 547−556.
38. Maddy, A. H. (1964) A fluorescent label for the outer components of the plamsa membrane, *Biochim. Biophys. Acta 880*, 390−399.
39. Knauf, P. A., and Brahm, J. (1989) Functional asymmetry of the anion exchange protein, capnophorin: effects on substrate and inhibitor binding, *Methods Enzymol. 173*, 432−453.
40. Knauf, P. A., Raha, N. M., and Spinelli, L. J. (2000) The noncompetitive inhibitor WW781 senses changes in erythrocyte anion exchanger (AE1) transport site conformation and substrate binding, *J. Gen. Physiol. 115*, 159−173.
41. Bicknese, S., Rossi, M., Thevenin, B. J., Shohet, S. B., and Verkman, A. S. (1995) Anisotropy decay measurement of segmental dynamics of the anion binding domain in erythrocyte band 3, *Biochemistry 34*, 10645−10651.
42. Laemmli, U. K. (1970) Cleavage of structural proteins during the assembly of the head of bacteriophage T4, *Nature 227*, 680−685.
43. Lieberman, D. M., and Reithmeier, R. A. F. (1983) Characterization of the stilbenedisulfonate binding site of the band 3 polypeptide of human erythrocyte membrane, *Biochemistry 22*, 4028−4032.
44. Knauf, P. A., Law, F.-Y., and Hahn, K. (1995) An oxonol dye is the most potent known inhibitor of band 3-mediated anion exchange, *Am. J. Physiol. (Cell Physiol.) 269*, C1073−C1077.
45. Dale, R. E., Eisinger, J., and Blumberg, W. E. (1979) The orientational freedom of molecular probes. The orientation factor in intramolecular energy transfer, *Biophys. J. 26*, 161−194.
46. Förster, T. (1959) Transfer mechanisms of electronic excitation, *Discuss. Faraday Soc. 27*, 7−17.
47. Arnold, B. R., Atherton, S. J., Farid, S., Goodman, J. L., and Gould, I. R. (1997) Combined application of picosecond transient absorption and emission measurements in studies of radical-ion pair dynamics, *Photochem. Photobiol. 65*, 15−22.
48. Birch, D. J. S., and Imhof, R. E. (1991) Time-domain fluorescence spectroscopy using time-correlated single-photon counting, in *Topics in Fluorescence Spectroscopy* (Lakowicz, J. R., Ed.) pp 1−95, Plenum Press, New York.
49. Lakowicz, J. R. (1999) *Principles of Fluorescence Spectroscopy*, Kluwer Academic/Plenum Publishers, New York.
50. Lakowicz, J. R. (1983) *Principles of Fluorescence Spectroscopy*, Plenum Press, New York.
51. Hillel, Z., and Wu, C.-W. (1976) Statistical interpretation of fluorescence energy transfer measurements in macromolecular systems, *Biochemistry 15*, 2105−2113.
52. Casey, J. R., and Reithmeier, R. A. F. (1991) Analysis of the oligomeric state of band 3, the anion transport protein of the human erythrocyte membrane, by size exclusion high performance liquid chromatography. Oligomeric stability and origin of hetrogeneity, *J. Biol. Chem. 266*, 15726−15737.
53. Salhany, J. M., Cordes, K. A., and Sloan, R. L. (2000) Mechanism of band 3 dimer dissociation during incubation of erythrocyte membranes at 37 °C, *Biochem. J. 345*, 33−41.

54. Blackman, S. M., Piston, D. W., and Beth, A. H. (1998) Oligomeric state of human erythrocyte band 3 measured by fluorescence resonance energy homotransfer, *Biophys. J. 75*, 1117−1130.
55. Janas, T., Bjerrum, P. J., Brahm, J., and Wieth, J. O. (1989) Kinetics of reversible DIDS inhibition of chloride self-exchange in human erythrocytes, *Am. J. Physiol. (Cell Physiol.) 257*, C601−C606.
56. Thevenin, B. J., Periasamy, N., Shohet, S. B., and Verkman, A. S. (1994) Segmental dynamics of the cytoplasmic domain of erythrocyte band 3 determined by time-resolved fluorescence anisotropy: sensitivity to pH and ligand binding, *Proc. Natl. Acad. Sci. U.S.A. 91*, 1741−1745.
57. Thevenin, B. J., Willardson, B. M., and Low, P. S. (1989) The redox state of cysteines 201 and 317 of the erythrocyte anion exchanger is critical for ankyrin binding, *J. Biol. Chem. 264*, 15886−15892.
58. Leenders, R., Roslund, J., and Visser, J. W. G. (1995) Time-resolved tryptophan fluorescence in flavodoxins, *J. Fluoresc. 5*, 349−353.
59. Jia, Y., Sytnik, A., Li, L., Vladimirov, S., Cooperman, B. S., and Hochstrasser, R. M. (1997) Nonexponential kinetics of a single tRNAPhe molecule under physiological conditions, *Proc. Natl. Acad. Sci. U.S.A. 94*, 7932−7936.
60. Cobb, C. E., and Beth, A. H. (1990) Identification of the eosinyl-5-maleimide reaction site on the human erythrocyte anion-exchange protein: overlap with the reaction sites of other chemical probes, *Biochemistry 29*, 8283−8290.
61. Thevenin, B. J., Bicknese, S. E., Verkman, A. S., and Shohet, S. B. (1996) Distance between Cys-201 in erythrocyte band 3 and the bilayer measured by single-photon radioluminescence, *Biophys. J. 71*, 2645−2655.
62. Zhang, D., Kiyatkin, A., Bolin, J. T., and Low, P. S. (2000) Crystallographic structure and functional interpretation of the cytoplasmic domain of erythrocyte membrane band 3, *Blood 96*, 2925−2933.
63. Zhou, J., and Low, P. S. (2001) Characterization of the reversible conformational equilibrium in the cytoplasmic domain of human erythrocyte membrane band 3, *J. Biol. Chem. 276*, 38147−38151.
64. Bahar, S., Gunter, C. T., Wu, C., Kennedy, S. D., and Knauf, P. A. (1999) Persistence of external chloride and DIDS binding after chemical modification of Glu-681 in human band 3, *Am. J. Physiol. (Cell Physiol.) 277*, C791−C799.
65. Tang, X.-B., Fujinaga, J., Kopito, R., and Casey, J. R. (1998) Topology of the region surrounding Glu^{681} of human AE1 protein, the erythrocyte anion exchanger, *J. Biol. Chem. 273*, 22545−22553.
66. Jennings, M. L., and Anderson, M. P. (1987) Chemical modification and labeling of glutamate residues at the stilbenedisulfonate site of human red blood cell band 3 protein, *J. Biol. Chem. 262*, 1691−1697.
67. Jennings, M. L., and Al-Rhaiyel, S. (1988) Modification of a carboxyl group that appears to cross the permeability barrier in the red blood cell anion transporter, *J. Gen. Physiol. 92*, 161−178.
68. Jennings, M. L., and Smith, J. S. (1992) Anion-proton cotransport through the human red blood cell band 3 protein: role of glutamate 681, *J. Biol. Chem. 267*, 13964−13971.
69. Jennings, M. L. (1995) Rapid electrogenic sulfate-chloride exchange mediated by chemically modified band 3 in human erythrocytes, *J. Gen. Physiol. 105*, 21−47.
70. Sekler, I., Lo, R. S., and Kopito, R. R. (1995) A conserved glutamate is responsible for ion selectivity and pH dependence of the mammalian anion exchangers AE1 and AE2, *J. Biol. Chem. 270*, 28751−28758.
71. Tang, X.-B., and Casey, J. R. (1999) Trapping of inhibitor-induced conformational changes in the erythrocyte membrane anion exchanger AE1, *Biochemistry 38*, 14565−14572.
72. Canfield, V. A., and Macey, R. I. (1984) Anion exchange in human erythrocytes has a large activation volume, *Biochim. Biophys. Acta 778*, 379−384.
73. Cha, A., Snyder, G. E., Selvin, P. R., and Bezanilla, F. (1999) Atomic scale movement of the voltage-sensing region in a potassium channel measured via spectroscopy, *Nature 402*, 809−813.
74. Glauner, K. S., Mannuzzu, L. M., Gandhi, C. S., and Isacoff, E. Y. (1999) Spectroscopic mapping of voltage sensor movement in the *Shaker* potassium channel, *Nature 402*, 813−817.
75. Jennings, M. L., and Passow, H. (1979) Anion transport across the erythrocyte membrane, in situ proteolysis of band 3 protein, and cross-linking of proteolytic fragments by 4,4′-diisothiocyanodihydrostilbene-2,2′-disulfonate, *Biochim. Biophys. Acta 554*, 498−519.

BI048622A